Contents lists available at ScienceDirect

Journal of Magnetism and Magnetic Materials

journal homepage: www.elsevier.com/locate/jmmm

Morphology and magnetic properties of FeCo nanocrystalline powder produced by modified mechanochemical procedure

A. Azizi [a,b], S.K. Sadrnezhaad [b,*], A. Hasani [c]

[a] Department of New Materials, Materials and Energy Research Center (MERC), P.O. Box 14155-4777, Tehran, Iran
[b] Center of Excellence for Production of Advanced Materials, Department of Materials Science and Engineering, Sharif University of Technology, P.O. Box 11155-9466, Tehran, Iran
[c] Department of Materials, Faculty of Engineering, University of Semnan, Semnan, Iran

ARTICLE INFO

ABSTRACT

Properties of FeCo nanocrystalline intermetallic powders prepared by salt-matrix hydrogen reduction of a milled Fe_2O_3–Co_3O_4 mixture were investigated. The product of 72 ks ball-milling at 350 rpm was $CoFe_2O_4$ nanopowder. Reduction of this powder for 3.6 ks by hydrogen at 750 °C resulted in the formation of $Fe_{0.67}Co_{0.33}$ stoichiometric compound. Scanning electron microscopy, electron dispersive spectrometry, X-ray diffraction and vibrating sample magnetometry were used to characterize the nanopowder. Using a salt-matrix (NaCl as a dispersion medium) resulted in the decrease of the reduction temperature and improvement of the morphology and magnetic properties of the nanopowder. Dispersion of the ball-milled product in Hexan resulted in further improvements of the magnetic properties.

© 2010 Elsevier B.V. All rights reserved.

1. Introduction

FeCo intermetallic compound is a soft magnetic material of great importance due to unique properties such as large permeability, high Curie temperature and large saturation magnetization [1]. FeCo nanocrystals are building blocks of many magnetic materials and thin films [2–4]. They can also be used in biomedical systems [5]. Magnetic properties of nanostructured materials are affected by their microstructure, grain size, internal strain and crystal symmetry in a complicated manner [6,7]. Nanostructural control during FeCo synthesis is hence crucially significant in magnetic property improvements. Previous investigations have indicated mechanochemical milling followed by hydrogen reduction of the oxide powders as a good way for production of nanosized metallic particles [8]. This method has inspired operation for production of large quantities of nanostructured powders in a short period of time. Subsequent reduction can then release the milling strains possibly remaining in the samples [9]. Many researchers have tried to develop simple, efficient and cost effective methods for synthesizing nanoparticles with desirable morphology, structure and magnetic behavior. Suitable synthesis recipes have, for example, been devised by authors to produce nanoparticles with alternative morphologies and magnetic properties in low-temperature hydrogen-reduced mechanically alloyed ferrite powders [10,11]. This paper reports on the salt matrix hydrogen-reduction of $CoFe_2O_4$ fine particles as an attractive method for synthesis of morphology-controlled FeCo nanocrystallite powder. The procedure ends up producing FeCo nanoparticles of improved magnetic properties via a low-temperature reduction procedure.

2. Experimental method

Analytical grade hematite (Fe_2O_3; MERCK, Gmbh) was mixed with cobalt oxide (Co_3O_4; MERCK, Gmbh) at the elemental Fe:Co molar ratio of 2:1. The mixture was milled at 350 rpm via a planetary ball mill (RETSCH PM400, Gmbh), having a ball to powder weight ratio of 20:1 for 72 ks. The direction of rotation was changed each 7.2 ks. The produced Co-ferrite powder was then reduced with hydrogen. This was called sample A.

Sample B was produced by hydrogen reduction in the presence of NaCl as a dispersion medium. Chemical stability and water solubility of NaCl helped both reduction progression and eventual NaCl removal from the mixture. NaCl was first ball-milled for 72 ks to reduce its particle size and then mixed with the milled cobalt-ferrite powder. The mixture was then reduced with hydrogen. The as-milled $CoFe_2O_4$/NaCl weight ratio was 1:4.

Third set of the experiment was performed by separate dispersion in Hexan of the as-milled Co-ferrite and NaCl powders. The $CoFe_2O_4$/NaCl mixtures were stirred until all solvents evaporated before hydrogen reduction. This was called sample C.

* Corresponding author.
Tel.: +982166165215; fax: +982166005717.
E-mail address: sadrnezh@sharif.edu (S.K. Sadrnezhaad).

High-purity hydrogen was produced by a hydrogen generator and then mixed with gaseous argon coming from a high purity (99.9999%) argon cylinder. The hydrogen/argon ratio was adjusted at 9:1 and was flown over the sample placed within a tube-furnace used for hydrogen reduction. The rate of the gas flow was adjusted at 50 cm^3/min and the furnace was gradually heated up at the rate of 10 °C/min. When the furnace reached the predetermined reduction temperature, the holding time was set at 3.6 ks.

The optimum temperature was obtained by repetition of the experiments at different temperatures. It was found to be 750 °C for hydrogen reduction of the as-milled CoFe$_2$O$_4$ powder (sample A), while it was 650 °C for the milled CoFe$_2$O$_4$/NaCl powders without or with Hexan dispersion (samples B or C, respectively). The powders were centrifuge-washed several times with de-ionized water and methanol to remove all NaCl remains. X-ray diffraction patterns were taken by XRD (Philips PW 3710, Netherlands) to identify the phases present in the samples. Microstructural characteristics like morphology, particle size and composition of the reduced phase were investigated by scanning electron microscope (SEM, Philips XL30, Netherlands) equipped with energy dispersive X-ray spectrometer (EDX). Magnetic properties of the samples were measured by a vibrating sample magnetometer (VSM, I.R. Iran) at room temperature.

3. Results and discussion

Fig. 1 shows the XRD patterns of the as-milled, milled/reduced in the presence of NaCl and milled/reduced in the presence of NaCl with prior Hexan treatment. All observable peaks of Fig. 1a belong to single cobalt ferrite spinel produced via ball-milling of the raw powder mixture. No other phase can be seen in the figure. The broadness of the XRD peaks indicate decrease in crystallite size and increase in internal lattice strains due to mechanical milling of the sample. The solid–solid reaction of the raw materials to produce cobalt ferrite by ball-milling was according to the following reduction reaction:

$$Fe_2O_3(s) + (1/3)Co_3O_4(s) \rightarrow CoFe_2O_4(s) + (1/6)O_2(g) \qquad (1)$$
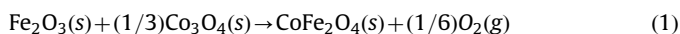
Ball-milled cobalt ferrite (CoFe$_2$O$_4$) was isothermally reduced by hydrogen at different temperatures. Fig. 1b reveals that the reduction process has not been completed at 650 °C and some peaks of cobalt ferrite are still visible. The reduction process was completed after increasing the temperature to 750 °C (Fig. 1c).
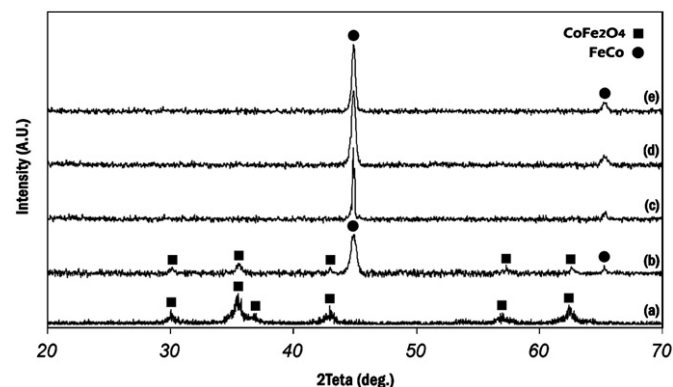

Fig. 1. X-ray diffraction pattern of powders after (a) 20 h milling, (b) hydrogen reduction of the as-milled sample at 650 °C, (c) hydrogen reduction of the as-milled sample at 750 °C, (d) hydrogen reduction of the mixture of the as-milled powder with NaCl at weight ratio of 1:4 and 650 °C and (e) hydrogen reduction of the Hexan treated mixtures of the milled CoFe$_2$O$_4$ and Nacl powders at weight ratio of 1:4 and 650 °C.

The observable peaks belonged to the single FeCo intermetallic phase having BCC structure, as is identified in Fig. 1c. Decrease in the peak's width could be the result of two phenomena: (a) increase in particle size and (b) release of internal lattice strain. As is identified in Fig. 1d and e, addition of NaCl results in lowering of reduction temperature without any distinct loss in the FeCo intermetallic phase formation.

As concluded in two previous papers by the same authors [10,11], mechanical alloying could contribute to diminishing of reduction temperature due to lattice strains induced during milling of the powders, which greatly affect the constitution and transformation of the ferrite phase [12]. Mechanical alloying was shown to reduce the reduction temperature of conventional nickel ferrite from 1100 to 600 °C [11,13]. Adding other novelties could result in further decrease in reduction temperature and achievement of additional improvements in the reduction conditions. An interesting effect was grain growth suppression, which happened only by NaCl (an inexpensive material) addition. No NaCl peak was observed after water/methanol centrifugal wash out in the XRD patterns (Fig. 1c and d). This meant that nearly all the salt was removed by the water/methanol centrifugal treatment. Average grain sizes calculated from the XRD patterns using the Scherrer formula [14] showed 25, 50, 30 and 37 nm for the as-milled, hydrogen reduced, hydrogen reduced with NaCl assistance and hydrogen reduced with NaCl assistance and prior Hexan treatment, respectively.

Typical SEM microstructures of the milled and milled–reduced samples are shown in Fig. 2. Huge surface free energy of the as-milled particles results in intense agglomeration and mechanical locking of the particles, as seen in Fig. 2a. The SEM image of the milled and 750 °C-reduced sample is shown in Fig. 2b. Comparison of Fig. 2a and b indicates that particle sizes considerably increase during hydrogen reduction similar to the results of Lee et al. [15]. Huge sintering of large particles can also occur as a result of welding and growth of particles during reduction. This intensive agglomeration may be due to high surface energies of small particles induced by mechanical alloying of the sample. The thermodynamic driving force for diffusion of reduced atoms acts during the reduction reaction. The reduced atoms can clearly diffuse from the highly strained lattice sites towards strain-free annealed positions. Similar results related to sintering and intense growth of mechanically alloyed particles during hydrogen reduction have also been presented in the previous publications [10,11].

Salt matrix is used in this research to prevent huge agglomeration and grain-growth of the nanocrystalline particles. As seen in Fig. 2c, the NaCl addition has contributed to the prevention of growth of the particles to suppress creation of large agglomerates. Fine particles are, thus, majorly observable in the picture. It can be seen from Fig. 2d that the third process (prior treatment with Hexan of the CoFe$_2$O$_4$ milled with NaCl) has stronger effect in the prevention of agglomeration and possibility of grain growth of the powder. The average sizes of the particles embedded within the grains—determined by statistical analysis of SEM images—are lower than 100 nm.

Formation of finely dispersed FeCo nanoparticles by the devised process can thus be anticipated according to the following mechanism: NaCl acts as a dispersion medium to facilitate the completion of CoFe$_2$O$_4$ reduction and prevention of FeCo growth during high temperature sintering and heat treatment. Hou et al. [16] have stated facilitation of the reduction process of the oxide particles when oxide nanoparticles are well dispersed into the metallic reducers. A low cooling rate can then result in the relatively grown-up particles. In our modified process, the reduced nanoparticles are simply trapped within a solid-salt template, preventing grain-growth during sintering of the
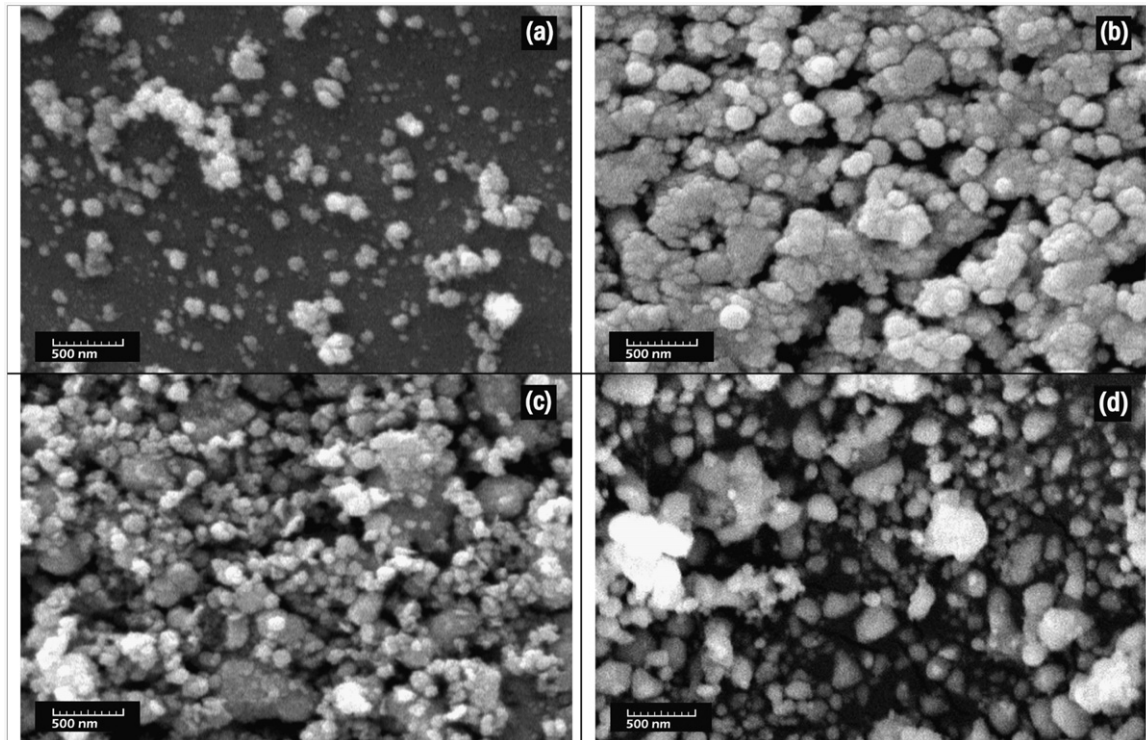
Fig. 2. SEM image of (a) 72 ks milled sample, (b) milled–750 °C-reduced sample, (c) reduced at 650 °C in the presence of NaCl at 1:4 weight ratio and (d) reduced at 650 °C in the presence of NaCl at 1:4 weight ratio and Hexan prior dispersion.
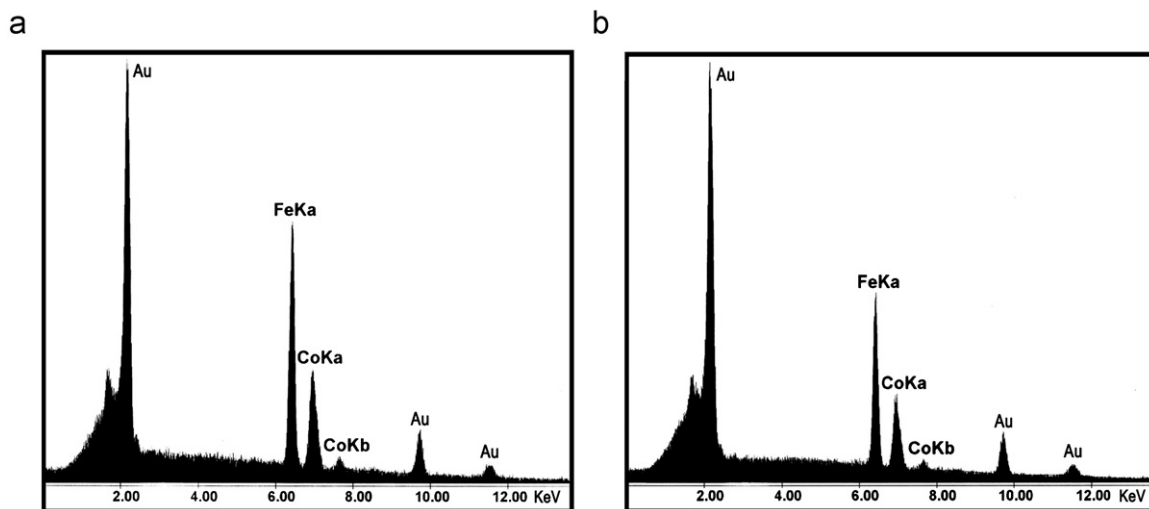

Fig. 3. EDX spectra of (a) the sample B reduced at 650 °C in the presence of NaCl at weight ratio of 1:4 and (b) the sample C-reduced at 650 °C in the presence of NaCl at weight ratio of 1:4 plus Hexan prior dispersion.

nanoparticles [17]. Hexan is also used to obtain a homogeneous salt–$CoFe_2O_4$–Hexan blend. Stirring results in solution saturation followed by precipitation. Well-dispersed mixture of the salt and $CoFe_2O_4$ is located within a furnace to bear the reduction reaction and subsequent cool-down treatment. Hexan is easily removed by warm-up evaporation.

Experimental results show that a finely dispersed FeCo nanopowder is obtained after removal of the salt by several washing–drying cycles. More salt may help the complete prevention of probable grain enlargement and sintering during the heat up process [18].

Fig. 3 shows the EDX spectra of samples C and D illustrated in parts c and d of Fig. 2, respectively. EDX results summarized in

Table 1 indicate $Fe_{0.67}Co_{0.33}$ stoichiometric formula for the reduced nanoparticles. The absence of NaCl in the samples is also nearly assessed (Fig. 3). This means that the whole salt can be removed by wash/centrifuging of the annealed mixture.

Magnetization curves of the milled–reduced and the as-milled samples are depicted in Fig. 4. Magnetic data such as saturation magnetization (M_s), coercivity (H_c) and remanent magnetization (M_r) for the milled–reduced and the as-milled samples are tabulated in Table 2. According to these data, saturation magnetization (M_s) of the as-milled nanocrystallite particles (42.0 emu/g) is much lower than that of the ideal nanocrystalline cobalt ferrite (~95 emu/g) powder. This can be attributed to domination of surface spin canting due to the

Table 1

EDX analyses of the images shown in Figs. 2c and d indicating stoichiometric formula $Fe_{0.67}Co_{0.33}$.

	Fe (at %)[a]	Co (at %)[a]	Fe (wt %)[a]	Co (wt %)[a]
Sample B	68.03	31.97	66.85	33.15
Sample C	67.54	32.46	66.35	33.65

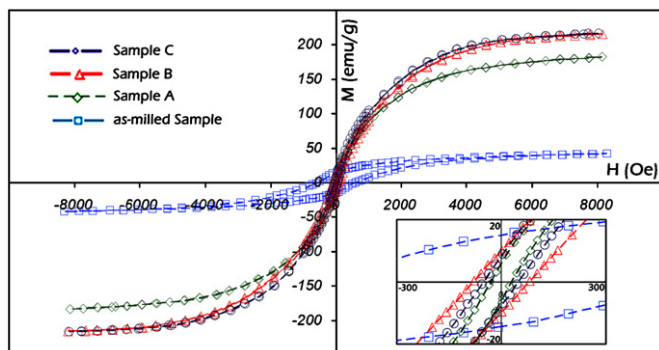[a] The amount of gold used for coating is excluded.

Fig. 4. Magnetization curves of the milled–reduced and the as-milled samples.

Table 2

Comparison of the magnetic data for the as-milled and the milled–reduced powders.

Sample	As-milled	Sample A	Sample B	Sample C
M_S (emu/g)	42.0	182.1	215.7	216.7
M_r (emu/g)	15.2	5.9	10.0	8.1
H_c (Oe)	607.5	35.6	77.9	55.1

mechanical milling over the cation sites exchange effect. Magnetization curves plotted in Fig. 4 clearly indicate magnetic properties of the samples produced in this research alter noticeably during the hydrogen reduction from semi-hard cobalt ferrite to soft FeCo performance. Details are as presented in Table 2.

Magnetic saturation is mainly related to structural arrangement of matter. M_s of the reduced samples is seen to be remarkably greater than that of the as-milled mixture, but not diverse for alternatively reduced nanopowders. The magnetic saturation reaches 216.7 emu/g for sample C. This number is noticeably larger than the corresponding value for sample A (Table 2).

M_S values of all reduced samples are, however, smaller than ∼245 emu/g of their bulk specimen [19]. This may be related to the slight oxidation of the powders during their wash-centrifuge treatment or due to the residual NaCl. Anisotropy of the surface/interface may be another reason. Large-pinning force resulting from surface/interface anisotropy may prevent magnetization of the layers close to the interface from rotating to the direction of the external field [19].

Coercivity of the products with the same structure is commonly related to morphology and especially to particle size of the powder. Previous researchers [20] have reported decrease of grain size down to values of about 40 nm resulting in increase

of H_c, irrespective of the kind of the mater. According to Zeng et al. [19], the increase of H_c is proportional to reciprocal of the grain size. The coercivities obtained in this research is also found to decrease from 77.9 Oe for sample B to 55.1 Oe for sample C and 35.6 Oe for sample A, in line with the enhancement of FeCo crystallite size in the samples. Besides, it is commonly reported that the ordered FeCo alloy with BCC structure illustrates low coercivity and good permeability in comparison with that of disordered structure resulting from directly milled materials (∼97 Oe) [15,21].

4. Conclusions

$Fe_{0.67}Co_{0.33}$ nanocrystalline intermetallic powder was produced by hydrogen reduction of the as-milled Co-ferrite sample at 750 °C for 3.6 ks. Reduced particles grew and welded together during hydrogen reduction. The optimum reduction temperature decreased from 750 to 650 °C by salt-matrix application. Using NaCl culminated in grain growth prevention and large agglomerates creation. Magnetic properties of the reduced samples noticeably improved during salt-matrix reduction. Hydrogen reduction of the in-Hexan dispersed as-milled powders together with NaCl resulted in more homogeneous blending and soft magnetic property improvement.

References

[1] T. Sourmail, Prog. Mater. Sci. 50 (2005) 816–880.
[2] H. Zeng, J. Li, J.P. Liu, Z.L. Wang, S. Sun, Nature 420 (2002) 395–398.
[3] H. Zeng, J. Li, Z.L. Wang, J.P. Liu, S. Sun, Nano Lett. 4 (2004) 187–190.
[4] R.S. Sunder, S.C. Deevi, Int. Mater. Rev. 50 (2005) 157–192.
[5] S. Behrens, H. Bönnemann, N. Matoussevitch, A. Gorschinski, E. Dinjus, W. Habicht, J. Bolle, S. Zinoveva, N. Palina, J. Hormes, H. Modrow, S. Bahr, V. Kempter, J. Phys.: Condens. Matter 18 (2006) S2543–S2561.
[6] A. Azizi, H. Yoozbashizadeh, A. Yourdkhani, M. Mohammadi, J. Magn. Magn. Mater. 322 (2010) 56–59.
[7] A. Azizi, S.K. Sadrnezhaad, Ceram. Int., in press, doi:10.1016/j.ceramint.2010.06.004.
[8] C. Suryanarayana, Prog. Mater. Sci. 46 (2001) 1–184.
[9] H.J. Fecht, Nanostruct. Mater. 6 (1995) 33–42.
[10] A. Azizi, H. Yoozbashizadeh, S.K. Sadrnezhaad, J. Magn. Magn. Mater. 321 (2009) 2729–2732.
[11] A. Azizi, S.K. Sadrnezhaad, J. Alloys. Compd. 485 (2009) 484–487.
[12] K. Gheisari, S. Javadpour, J.T. Oh, M. Ghaffari, J. Alloys. Compd. 472 (2009) 416–420.
[13] M. Bahgat, M.K. Paek, J.J. Pak, J. Alloys. Comp. 466 (2008) 59–66.
[14] A.L. Patterson, Phys. Rev. 56 (1939) 978–982.
[15] B. -H. Lee, B.S. Ahn, D. -G. Kim, S. -T. Oh, H. Jeon, J. Ahn, Y.D. Kim, Mater. Lett. 57 (2003) 1103–1107.
[16] Y. Hou, S. Sun, C. Rong, J.P. Liu, Appl. Phys. Lett. 91 (2007) 153117.
[17] X. Zhang, W. Jiang, D. Song, H. Sun, Z. Sun, F. Li, J. Alloys. Comp. 475 (2009) L34–L37.
[18] D. Li, N. Poudyal, V. Nandwana, Z. Jin, K. Elkins, J.P. Liu, J. Appl. Phys. 99 (2006) 08E911.
[19] Q. Zeng, I. Baker, V. McCreary, Z. Yan, J. Magn. Magn. Mater. 318 (2007) 28–38.
[20] D.S. Mathew, R.S. Juang, Chem. Eng. J. 129 (2007) 51–65.
[21] Z. Turgut, J.H. Scott, M.Q. Huang, S.A. Majetich, M.E. Mchenry, J. Appl. Phys. 83 (1998) 6468–6470.